Journal of Electronic Testing (2024) 40:679–687
https://doi.org/10.1007/s10836-024-06144-4

RESEARCH

Reliability Analysis for a GaAs LNA with Temperature Stress

Qian Lin[1,2,3] · **Mei-qian Wang**[1]

Received: 31 May 2024 / Accepted: 1 October 2024 / Published online: 21 October 2024

Abstract
In order to investigate the reliability of gallium arsenide (GaAs) monolithic microwave integrated circuit (MMIC) low noise amplifier (LNA), a series of tests have been carried out here. The results show that with the rising temperature the small-signal gain (S_{21}) decreases about 0.72 dB, output power Pout, gain and third-order intersection point (OIP3) with the reduction of 3.74 dB, 3.84 dB and 6.13 dB at 0.75 GHz, respectively. In addition, when the cycle number increase from 1 to 5, various indicators have been significantly decreased. Among them, there are some decrease of 0.79 dB, 4.88 dB and 4.99 dB for S_{21}, Pout and gain at -40 ℃ ~ 110 ℃, and 0.59 dB, 4.35 dB and 4.58 dB are dropped at -5 ℃ ~ 55 ℃. Moreover, all indicators decrease 3% with the increasing cycles. The detailed analysis shows that the degradation of LNA performance is closely related to the temperature, which provides an important theoretical basis and practical guidance for further optimizing the design of LNA and improving its reliability.

Keywords Temperature · Reliability · Low noise amplifier · Gallium arsenide

1 Introduction

As the key component of the RF front-end, the low noise amplifier (LNA) plays a crucial role in fields of aerospace [1], radio astronomy [2], wireless communications [3, 4] and radar [5, 6]. Generally, it is used to enhance the strength of the weak signals received from the antenna. Thus, its performance directly affects the noise and sensitivity of the receiver [7]. Therefore, the reliability of LNA is required to be higher with the continuous progress in communication technology.

In recent years, many scholars have achieved significant results for LNA development. In 2014, Yahaya designed a LNA with noise figure (NF) of less than 0.7 dB based on a negative feedback topology [8]. In 2015, Nikandish proposed a transformer feedback (TRFB) technique for wideband multistage amplifiers that can enhance the bandwidth within certain chip area and power consumption [9]. In 2016, he also introduced a design technique of wideband multistage LNAs with gain of 21.6 dB and NF of 1.8–2.7 dB for 18–43 GHz [10]. In 2017, Park implemented a high linearity LNA which significantly enhanced linearity and gain based on the improved common source and common gate structure [11]. In 2018, Memioglu achieved a two-stage design with the NF below 3.5 dB using the parallel feedback circuit [12]. In the 2020s, ultra-wideband and multiband switchable features are the new trend for LNAs. For example, Sakalas suggested an ultra-wideband LNA that can cover 4–42.5 GHz and achieve a good balance within the small-signal gain (S_{21}) and NF in 2020 [13]. In 2021, Wang showed a multi-band switchable LNA that can be continuously tuned to cover the 5G millimetre-wave bands without costing noise performance [14]. In 2022, Yan used a novel coupled-line based positive feedback structure to design a high performance 10–43 GHz of LNA [15].

The above studies have made significant progress in terms of LNAs performance. However, most of the LNAs still have limitation for specific application scenarios with high reliability. Meanwhile, compared with gallium nitride (GaN), gallium arsenide (GaAs) has superior characteristics in terms of high frequency, high power and high temperature. It has

Responsible Editor: T. Xia

✉ Qian Lin
linqian@tju.edu.cn

[1] School of Physics and Electronic Information Engineering, Qinghai Minzu University, Xining 810007, China

[2] School of Electronic Science and Engineering, University of Electronic Science and Technology, Chengdu 610000, China

[3] Tong Fang Electronic Technology Company, JiuJiang 332000, China

been widely utilized in the design of microwave circuit [16]. However, the behavior of LNA is significantly impacted by changes in temperature, which can lead to degradation or failure [17, 18]. Therefore, it is important to investigate the temperature reliability of LNA to cope with the complex application occasions.

Nowadays, there are few studies for LNA reliability. In 2010, Qin characterized the temperature effects on the large signal of a LNA at room temperature (RT) and 77 K [19]. In 2019, Çağlar demonstrated that the performance of a complementary metal oxide semiconductor (CMOS) LNA was greatly influenced by temperature [20]. In 2021, Weinreb conducted series of experiments on the small signal and noise for a LNA at -40 ~ 40 ℃ [21]. In 2022, Zhou executed some tests for a LNA with different temperatures and humidities [22]. In the same year, Lin found the power consumption of a monolithic microwave integrated circuit (MMIC) LNA increased with the rising temperature [23]. However, there is no the systemic and comprehensive studies for the temperature reliability of the LNA.

Hence, to investigate the temperature reliability for a GaAs LNA, a series of temperature tests have been carried out here. The results show that the input return loss (S_{11}), small signal gain (S_{21}), output return loss (S_{22}), output power (Pout), gain and third-order intersection point (OIP3) all drop with rising temperature within the frequency band of 0.1–1.5 GHz. Furthermore, with increasing number of cycles, S_{11}, S_{21}, S_{22}, Pout, and gain all exhibited certain degree of degradation, and significantly decrease at -40 ℃ ~ 110 ℃, and exhibiting slight changes at -5 ℃ ~ 55 ℃. However, the overall changes within 3%.

The paper is organized as follows: principle of LNA is described in Section II, the test environment is described in Section III, as well as the detailed circuit. In Section IV, the test results are discussed. Finally, concluding remarks are given in Section V.

1.1 Circuit Design and Implementation

The schematic of the LNA and fixture are shown in Fig. 1. It can be seen that it is consisted of the input matching network, gate bias circuit, feedback amplification, interstage matching circuit, final amplification and output matching network. First, the LC series resonant circuit is adopted in the input matching network to achieve input impedance matching and improve signal transmission efficiency. Then, the gate bias circuit is composed of the resistors of R_1—R_5 and capacitors of C_3—C_4. Especially, the stacked transistors of M_1 and M_2 with cascade structure are utilized for the feedback amplification circuit. In detail, the cascode structure can reduce the influence of Miller effect of junction capacitance and expand the bandwidth. At the same time, it has the characteristics of high gain, wide bandwidth, good stability and high linearity. However, it also introduces certain nonlinearity and noise. The contribution of channel noise of M_2 to the NF is expressed as Eq. (1) [24]:

$$i_{o,d2} \approx \frac{\frac{1}{j\omega C_{gs}} + r_{o1}}{g_m \frac{1}{j\omega C_{gs}} r_{o1} + \frac{1}{j\omega C_{gs}} + r_{o1}} i_{d2} \tag{1}$$

where g_m is the transconductance, i_{nd} is the drain current, C_{gs} is equivalent capacitancethe for gate source and r_{o1} is the output resistance.

Assuming that the drain impedance of M_1 is only the output resistance r_{o1}, where $g_m r_{o1}$ is much larger than 1. Considering the low frequencies, ω is much smaller than ω_T, ω_T is the characteristic frequency, then it can be obtained the Eq. (2) [24]:

$$\overline{i_{o,d2}^2} \approx \left(\frac{1}{{g_m}^2 {r_{o1}}^2} + \frac{\omega^2}{\omega_T}\right)\overline{i_{d2}^2} << \overline{i_{d2}^2} \tag{2}$$

From the equation above, it can be seen that the noise contribution of the M_2 is much smaller than M_1, Then it can

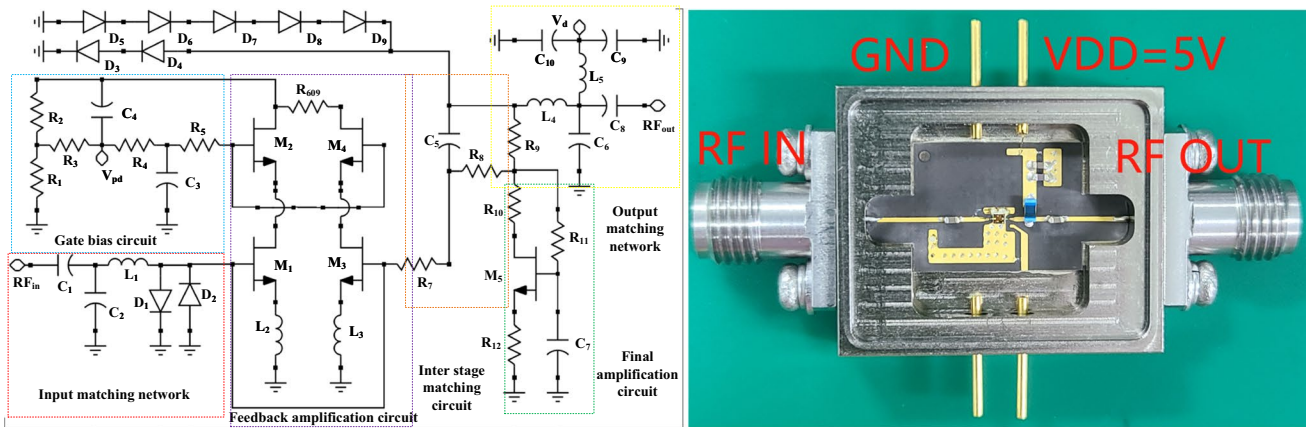

Fig. 1 Schematic of LNA (left) and fixture (right)

be assumed that M_1 and M_2 are disconnected and the noise generated by M_2 has little effect on the total output noise. Thus, the final noise can be obtained as Eq. (3) [24]:

$$F = 1 + \frac{\gamma}{\alpha g_{m1} R_S} \tag{3}$$

where γ is the thermal noise coefficient, α is the bulk charge coefficient and R_S is the internal resistance of the signal source. Whilst the stacked transistors of M_3-M_4 are connected in parallel to form the 2-stacked-FET amplifier. The common source stage is connected in series with the feedback inductors of L_2-L_3 to obtain optimal noise matching and input–output matching. Also, in order to suppress self-oscillation, the resistor of R_6 is connected in series between the transistors of M_2 and M_4. Moreover, the RC matching network with resistor of R_7 and capacitor of C_5 is designed to improve interstage impedance matching and frequency selection. In addition, in the final stage amplification circuit, the resistors of R_{12} and R_{10} are connected in series between transistors of M_5, the resistor of R_{11} and capacitor of C_7 are connected in parallel to form the common source stage of the common source and common gate structure, which can improve stability and suppress high-frequency noise. Then, two T-networks are connected in parallel, which can optimize signal transmission and reduce reflection loss. In addition, the diodes of D_1-D_9 are employed to enhance the reliability of LNA. Therefore, this LNA can be applied in wireless communication fields such as base station infrastructure, broadband wireless access systems, microwave radar and LTE equipment.

2 Test Preparation

The test environment and setup are shown in Fig. 2 and Fig. 3, respectively. It can be seen that the temperature chamber, DC source and vector network analyzer (VNA) are used here. DC source can provide the bias supply for LNA, and VNA is used to measure the S_{21}, S_{11}, S_{22} and RF output. Temperature chamber is employed to provide various temperatures. Additionally, to ensure the safety of VNA, an attenuator of 30 dB is also connected between the LNA and VNA.

First, In order to get the optimal work status, LNA is tested at different bias voltages of V_{gs}. Test curves of S_{21} at different V_{gs} is shown in Fig. 4. It can be observed that when V_{gs} is decreasing form 5.2 V to 3.3 V, the small signal of S_{21} shows an downward trend with the decrements of 0.61 dB.

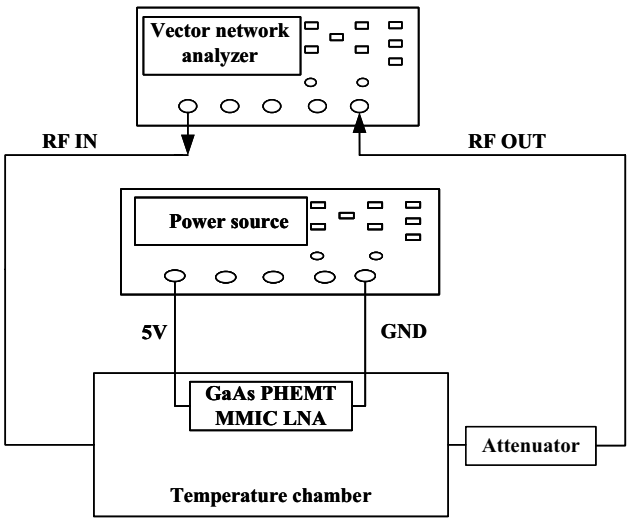

Fig. 3 Test setup of LNA

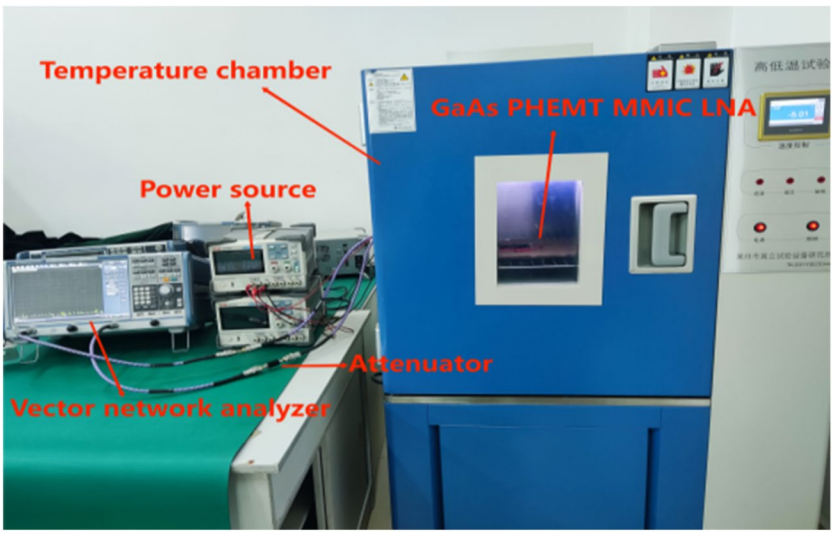

Fig. 2 Test environment of LNA

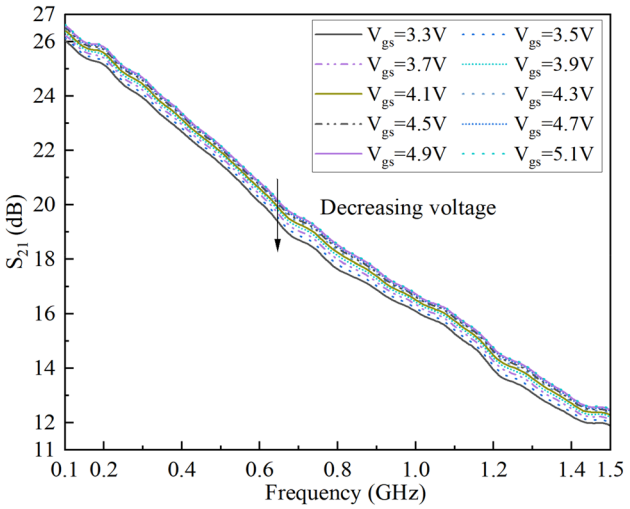

Fig. 4 Test curves of S_{21} for LNA at different voltages

It is reported that the on-resistance of R_{on} can represent the overall resistance between the source and drain contacts. It can be derived from Eq. (4) [25]:

$$R_{on} = R_0 + KT^{\alpha} / \left| V_{gs} - V_{th} \right|^{\beta} \tag{4}$$

where K is a technological parameter, T is temperature, V_{gs} is the gate bias voltage, V_{th} is the threshold voltage, α and β are 1.5 and 0.2, respectively. And R_0 is used to represent the contribution of R_{on} independent of V_{gs} and temperature. Generally, in order to obtain the lower g_m, V_{gs} should be lower. When $V_{gs} \gg V_{th}$, thus V_{th} can be ignored. Therefore, it can be deduced that R_{on} increases with the decreasing V_{gs}, which can lead to the decrement of I_{ds} and g_m.

Moreover, the test curves of Pout and gain for LNA at different V_{gs} are shown in Fig. 5. It can be observed that when V_{gs} decreases from 5.5 V to 3.3 V, the downward trends are presented for Pout and gain with the decrement of 4.62 dB and 1.32 dB, respectively.

To investigate the root cause, it can be shown that V_{gs} can be expressed as Eq. (5) [26]:

$$V_{gs} = V_T + \frac{2(1-\eta^{-0.5})L}{C_{ox} R w \mu} \tag{5}$$

where η is the channel width ratio, W is the gate width, L is the gate length, C_{ox} is the oxide layer capacitance between the gate and channel, μ is the two-dimensional electron–gas mobility, R is resistor, the influence of V_{th} can be ignored. The mobility μ can be obtained from the carrier concentration *N* by the following Eq. (6) [27]:

$$\mu = \mu_{n0} / (1 + \alpha N) \tag{6}$$

where N is the carrier concentration, α is the constant related to the material properties and μ_{n0} is the initial value of carrier mobility. When the influence of η, W, L, and C_{ox} can be ignored, it is clear that if V_{gs} and N decreases, then μ will increase. This means that when V_{gs} is low which can lead to the decrement for N. Thus, the probability of collision between electrons and holes in the high electric field, the energy transfer and scattering of electrons can be reduced. As a result, Pout and gain are decreased with V_{gs}.

Based on the results above, the optimal bias voltage of V_{gs} is set as 5.5 V. Then, this LNA is tested at RT to get the normal index. From Fig. 6 and Fig. 7, it can be observed that at the condition of RT, its S_{21} is greater than 12 dB, S_{11} and S_{22} are both less than -5 dB within the frequency band of 0.1–1.5 GHz. At once, its Pout is up to 21.5 dBm and gain is above 18.3 dB.

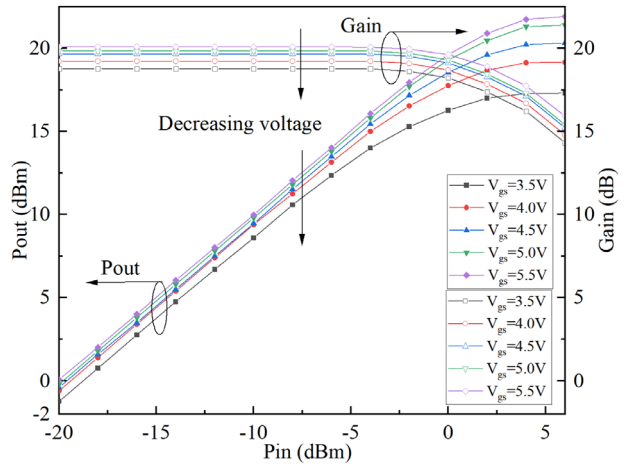

Fig. 5 Test curves of Pout and gain at different voltages

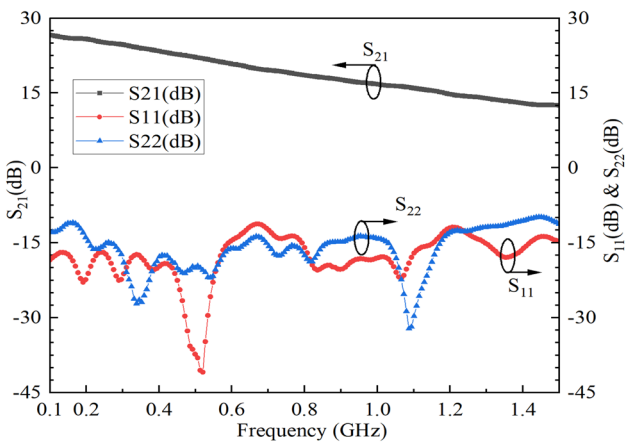

Fig. 6 Test curves of S_{21}, S_{11} and S_{22} for LNA at RT

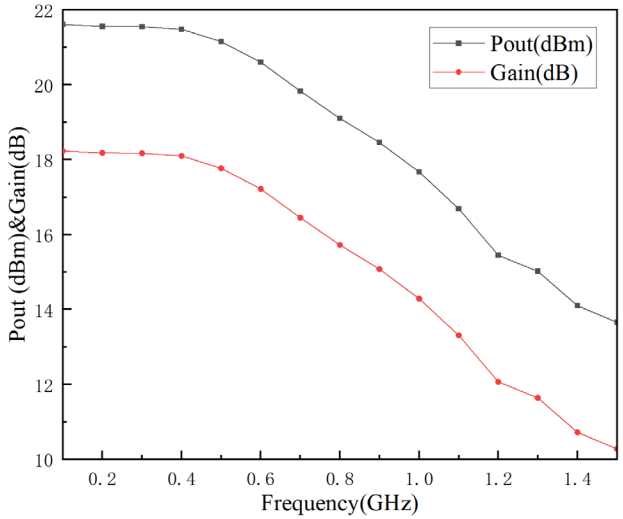

Fig. 7 Test curves of Pout and gain of LNA at RT

2.1 Test Results and Analysis

In order to study the temperature reliability of LNA with different temperatures, a series of tests have been carried out here. The test temperatures are chosen as -40 ℃, -5 ℃, 25 ℃, 55 ℃ and 110 ℃. Meanwhile, -40 ℃ ~ 110 ℃ and -5 ℃ ~ 55 ℃ are set for temperature cycles. During the tests, LNA is stored for 2 h and then powered on for 0.5 h.

2.1.1 Analysis of Temperature Testing

Test curves of S_{21}, S_{11} and S_{22} for LNA at different temperatures are shown in Fig. 8. It can be seen that within the frequency band of 0.1—1.5 GHz, S_{11}, S_{21} and S_{22} decrease about 2.21 dB, 0.72 dB, and 2.59 dB when temperature increases from -40 ℃ to 110 ℃, respectively.

It can be deduced from the truth that I_{ds} in various states can be expressed as Eq. (7) and (8) [28]:

I_{ds} in the linear region is expressed as follows:

$$I_{ds} = \frac{\mu w c_{ox}}{L_d}[(V_{gs} - V_{th})V_{ds} - \frac{V_{ds}^2}{2}] \tag{7}$$

I_{ds} in the saturation region is expressed as follows:

$$I_{ds} = \frac{\mu w c_{ox}}{2L_d}(V_{gs} - V_{th})^2 \tag{8}$$

where d is the thickness of the barrier layer, V_{ds} is the drain-source voltage and I_{ds} is the drain-source current.

Then, it is deduced that the transconductance (g_m) is expressed as Eq. (9) and (10) [27]:

The g_m in the linear region is as follows:

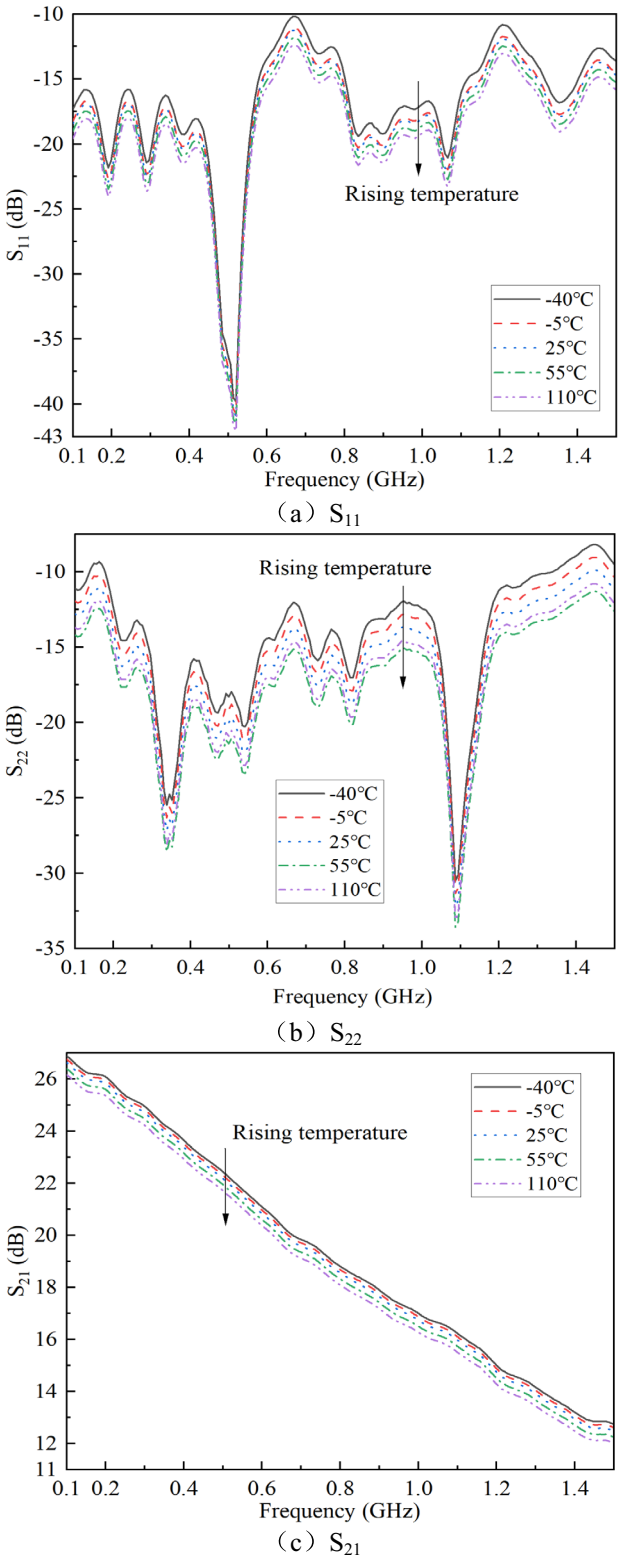

Fig. 8 Test curves of S_{21}, S_{11} and S_{22} for LNA at different temperatures. (a)S_{11}, (b)S_{22}, (c)S_{21}

$$g_m = \sqrt{2\mu \frac{wc_{ox}}{L} I_{ds}} \tag{9}$$

The g_m in the saturation region is as follows:

$$g_m = \sqrt{2\mu \frac{wc_{ox}}{L} I_{ds}} \tag{10}$$

The carrier mobility μ can be expressed by the Eq. (11) [29]:

$$\mu(T) = \mu(T_0)\left(\frac{T}{T_0}\right)^{-m} \tag{11}$$

where T_0 is 300 K, m is 1.5 ~ 2. According to (9)—(11), g_m is proportional to μ, and T is inversely proportional to μ. Therefore, g_m gradually decreases with the rising temperature. Moreover, g_m represents the advantages and disadvantages of grid control capability, and its value directly affects S_{21}, S_{11} and S_{22}. Thus, it shows a downward trend with the rising temperature.

In conclusion, the test curves of Pout and gain for LNA at different temperatures are shown in Fig. 9. It can be seen that when the temperature rises from -40 ℃ to 110 ℃, Pout decreases about 4.14 dB and gain drops about 4.15 dB at 0.75 GHz. When Pin is 0 dBm, its Pout and gain drop about 3.74 dB and 3.84 dB, respectively.

One of the most important parameters of any LNA is NF, the test curves of NF for this LNA at different temperatures are shown in Fig. 10. It can be seen that NF is less than 0.5 dB within the frequency band of 0.5—1.0 GHz at RT and NF is rising with the temperature. When the temperature rises from -40 ℃ to 110 ℃, it increases about 0.51 dB at 0.75 GHz.

Furthermore, linearity is particularly important for LNA. In order to investigate the varition of OIP3, the test curves of OIP3 for this LNA with different temperatures are shown in Fig. 11. It can be observed that its OIP3 gradually decreases with the rising temperature. When the temperature upto 110 °C, it drops about 6.13 dB at 0.75 GHz. This also can be concluded that its linearity is deteriorated dramatically with the rising temperature.

2.1.2 Analysis of Temperature Cycling Test

In order to study the temperature reliability for LNA with temperature mutation, several temperature cycles have been carried out. The cycling conditions are set to -40 ℃ ~ 110 ℃ and -5 ℃ ~ 55 ℃.

Thus, test curves of S_{21}, S_{11} and S_{22} with cycle numbers are shown in Fig. 12. Based on the results above, it can be seen that when the cycle number increase from 1 to 5, S_{21} decreases about 0.79 dB, S_{11} decreases about 0.48 dB, S_{22} decreases about 0.69 dB at -40 ℃ ~ 110 ℃, and

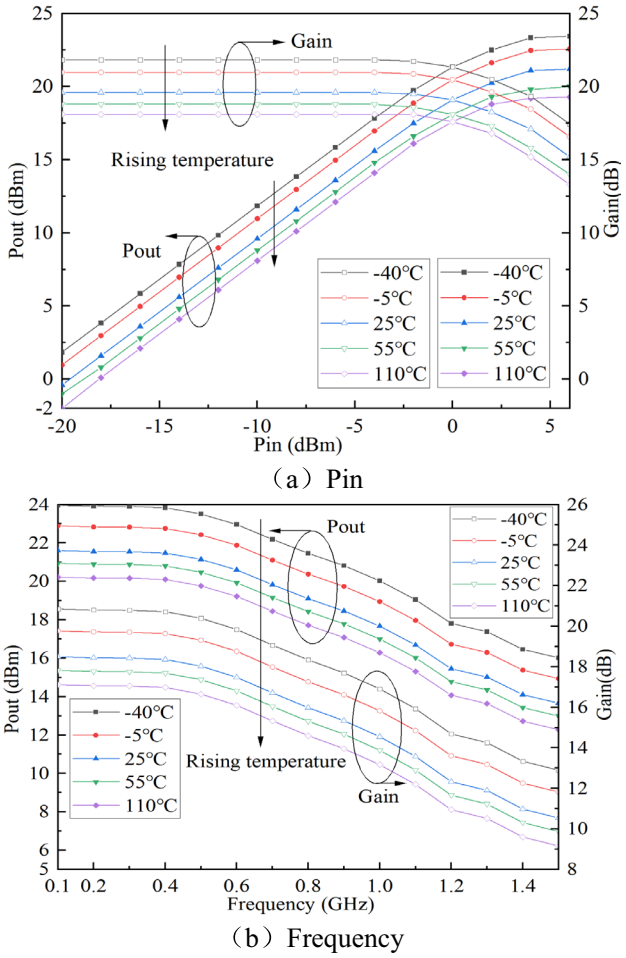

Fig. 9 Test curves of Pout and gain at different temperatures (**a**) Pin, (**b**) Frequency

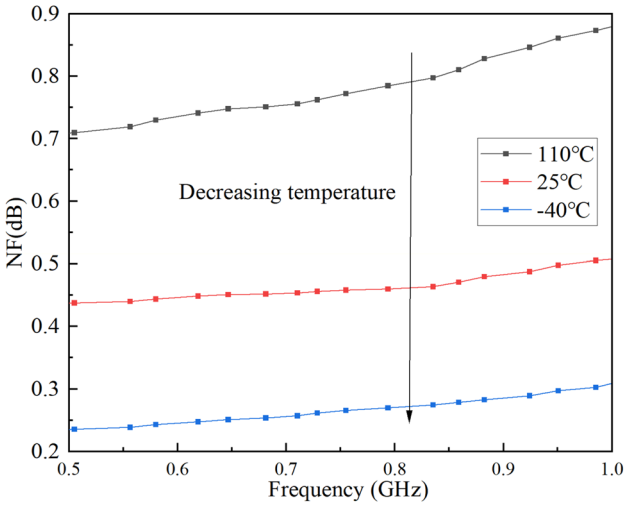

Fig. 10 Test curves of NF at different temperatures

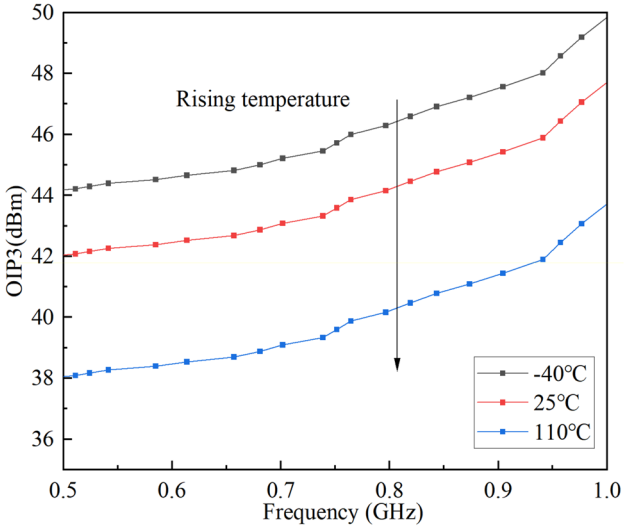

Fig. 11 Test curves of OIP3 at different temperatures

0.59, 0.72 and 0.46 dB are appeared at -5 ℃ ~ 55 ℃, respectively. Among them, the decrease is more pronounced at -40 ℃ ~ 110 ℃ than -5 ℃ ~ 55 ℃.

Then, when Pin is 0 dBm, test curves of Pout and gain with cycle numbers are shown in Fig. 13. It can be seen that a significant downward trend is presented for Pout and gain when the number of cycles increase. In detail, the Pout and gain drop about 4.88 dB and 4.99 dB at -40 ℃ ~ 110 ℃, and the Pout and gain drop about 4.35 dB and 4.58 dB at -5 ℃ ~ 55 ℃, respectively.

At the frequency of 0.75 MHz, test curves of Pout and gain with cycle numbers are shown in Fig. 14. It can be observed that Pout and gain show a degradation trend with the increasing cycle. Furthermore, this degradation becomes more serious as the cycle increases, and Pout and gain decrease 4.86 dB and 4.96 dB at -40 °C ~ 110 °C, respectively, and 4.65 dB and 4.71 dB at -5 °C ~ 55 °C, respectively. Additionally, the reliability is more affected by abrupt temperature. However, the variation range is approximately 3%.

3 Conclusion

In this paper, the temperature reliability of a GaAs LNA has been investigated experimentally. In detail, the S_{21}, S_{11} and S_{22}, Pout, gain, NF and OIP3 decrease significantly with the rising temperature. However, the cause of the degradation is that S_{21}, S_{11} and S_{22} degrades as the μ increases with temperature. Concurrently, the power consumption increases with the on-resistance of R_{on}, resulting in the decrease of Pout and gain. Furthermore, the indicators exhibit the downward trend with increasing

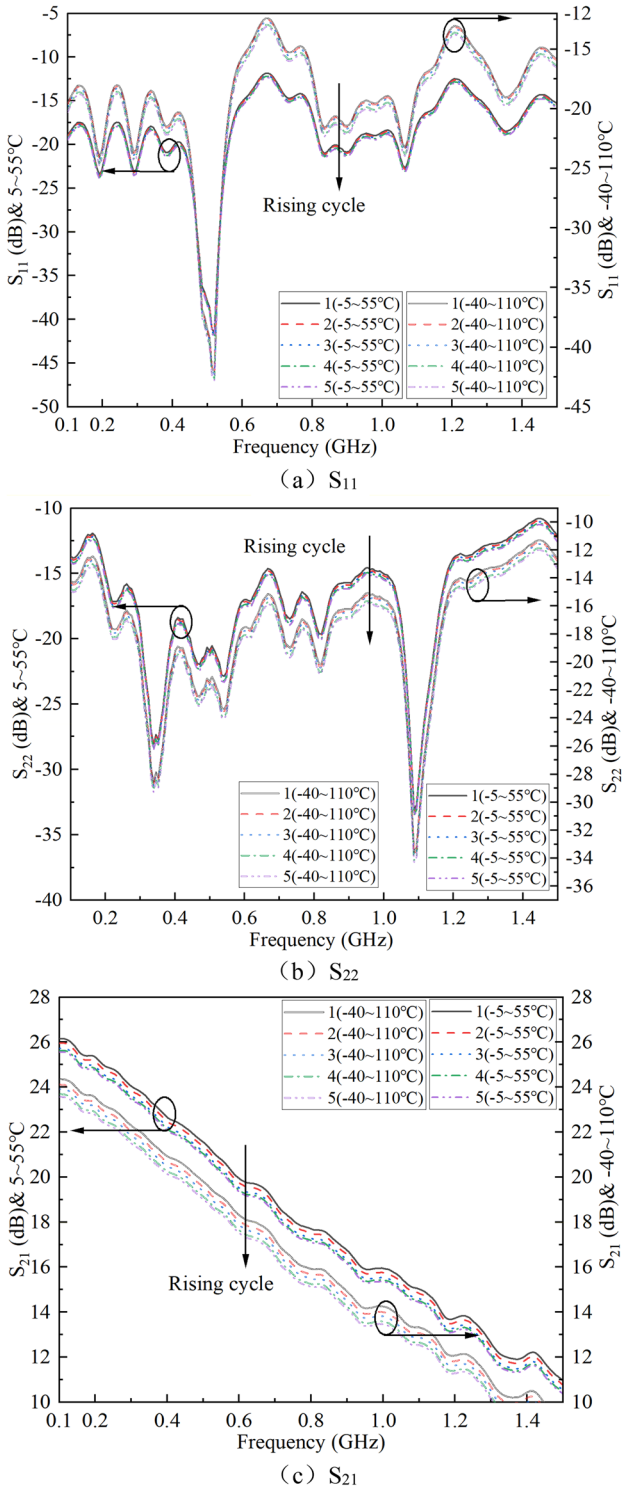

Fig. 12 Test curves of S_{21}, S_{11} and S_{22} with cycle numbers. (**a**) S11, (**b**) S22, (**c**) S21

temperature cycle number, and the overall changes about 3%. In summary, it demonstrates that temperature has a significant impact on the reliability of LNA, providing crucial experimental evidence for the design and optimization

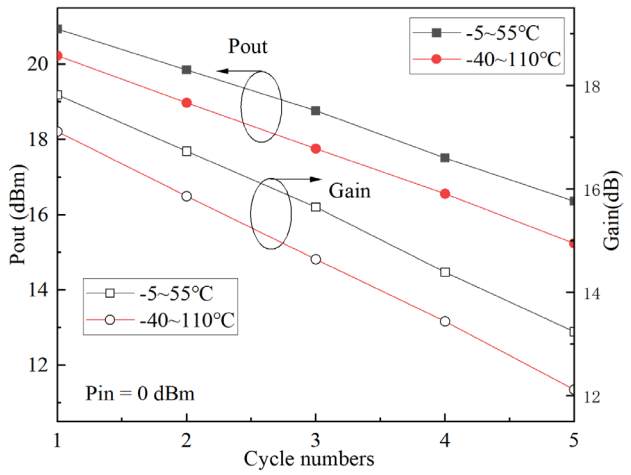

Fig. 13 Test curves of Pout and gain with cycle numbers

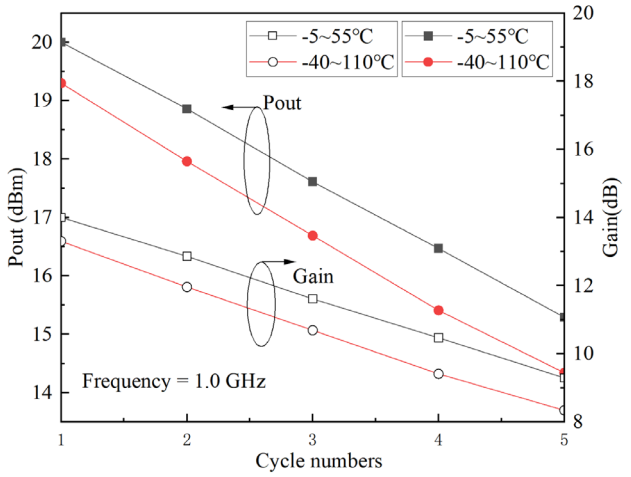

Fig. 14 Test curves of Pout and gain with cycle numbers at 0.75 GHz

of LNA. Specifically, in high stability and reliability, the influence of temperature factors on reliability of LNA must be fully considered.

Acknowledgements The authors gratefully acknowledge financial support by the National Natural Science Foundation (62161046), the West Light Youth Talent Program of the Chinese Academy of Sciences (1_14), and the Postdoctoral Project with University of Electronic Science and Technology and Tongfang Electronic Technology Company.

Author Contributions Methodology, Qian Lin; test, Meiqian Wang; data curation, Meiqian Wang; writing—original draft preparation, Meiqian Wang; visualization, Meiqian Wang; supervision, Qian Lin; funding acquisition, Qian Lin. All authors have read and agreed to the published version of the manuscript.

Data Availability The datasets generated during and/or analyzed during the current study are available from the corresponding author on reasonable request.

Declarations

Conflicts of Interest All authors certify that they have no affiliations with or involvement in any organization or entity with any financial interest or non-financial interest in the subject matter or materials discussed in this manuscript.

References

1. Rao CVN, Ghodgaonkar DK, Sharma N (2018) GaAs MMIC Low Noise Amplifier With Integrated High-Power Absorptive Receive Protection Switch. IEEE Microw Wirel Compon Lett 28(12):1128–1130
2. Jimenez-Martin JL, Gonzalez-Posadas V, Parra-Cerrada A, Garcia-Muñoz LE, Segovia-Vargas D (2019) Broadband (1–16 GHz) Balanced MMIC GaAs pHEMT LNA for Radio Astronomy Applications. European Microwave Conference in Central Europe (EuMCE), Prague, Czech Republic, pp 91–94
3. Slimane A, Trabelsi M, Belaroussi MT (2011) A 0.9-V, 7-mW UWB LNA for 3.1–10.6-GHz wireless applications in 0.18-µm CMOS technology. Microelectron J 42(11):1263–1268
4. Khodabakhsh A, Fallahnejad M, Vadizadeh M (2024) A breakthrough for temperature and linearity stability from device to circuit-level with 14 nm junctionless SOI FinFET: Advancing K-band LNA performance. Microelectron Reliab 152(1):115278–115290
5. Florian C, Traverso PA, Santarelli A (2021) A Ka-band MMIC LNA in GaN-on-Si 100-nm technology for high dynamic range radar receivers. IEEE Microwave Wirel Compon Lett 31(2):161–164
6. Girard M et al (2018) Effects of HPEM stress on GaAs low-noise amplifier from circuit to component scale. Microelectron Reliab 88–90(1):914–919
7. Çağlar A, Yelten MB (2019) Design of Cryogenic LNAs for High Linearity in Space Applications. IEEE Trans Circuits Syst I Regul Pap 66(12):4619–4627
8. Yahaya NZ, Yazid S, Osman A, Huzairi H (2014) Wideband low noise amplifier design for 2.3–2.4 GHz WiMAX application. Lecture Notes in Electrical Engineering, LNEE, pp 373–384
9. Nikandish G, Medi A (2015) Transformer-Feedback Interstage Bandwidth Enhancement for MMIC Multistage Amplifiers. IEEE Trans Microw Theory Tech 63(2):441–448
10. Nikandish G, Yousefi A, Kalantari M (2016) A Broadband Multistage LNA With Bandwidth and Linearity Enhancement. IEEE Microw Wirel Compon Lett 26(10):834–836
11. Park SP, Lee MQ, Lee HL (2017) Wideband highly linear LNA using modified cascode for simultaneous input and noise matching technique. Microw Opt Technol Lett 59(1):15–17
12. Memioglu O, Gundel A (2018) "A High Linearity Broadband Gain Block/LNA MMIC with Diode Predistortion in GaAs pHEMT Technology", 18th Mediterranean Microwave Symposium (MMS). Istanbul, Turkey, pp 120–123
13. Sakalas M, Sakalas P (2020) Design of a wideband, 4 – 42.5 GHz Low Noise Amplifier in 0.25 µm GaAs pHEMT Technology. IEEE BiCMOS and Compound Semiconductor Integrated Circuits and Technology Symposium (BCICTS), Monterey, CA, USA, pp 1–4
14. Wang Z et al (2021) A Ka-Band Switchable LNA With 2.4-dB NF Employing a Varactor-Based Tunable Network. IEEE Microw Wireless Compon Lett 31(4):385–388
15. Yan X, Yu P, Zhang J, Gao S-P, Guo Y (2022) A Broadband 10–43-GHz High-Gain LNA MMIC Using Coupled-Line Feedback in 0.15-µm GaAs pHEMT Technology. IEEE Microwave Wirel Compon Lett 32(12):1459–1462

16. Wu HF, Yang RL, Wang MQ, et al (2022) A Low-Noise, High-Linearity Amplifier for Wireless Base-Stations. 7th International Conference on Integrated Circuits and Microsystems (ICICM), Xi'an, China, pp 340–344
17. Lin Q, Jia LN, Wu HF et al (2022) Investigation on Temperature Behavior for a GaAs E-pHEMT MMIC LNA. Micromachines 13(7):1121–1131
18. Khodabakhsh A, Amini A, Fallahnejad M (2024) Highly Linear and Low Noise Shell Doped GaN Junctionless Nanotube TeraFET for the Design of Ultra-Wideband LNA in 6G Communications. IEEE Trans Nanotechnol 23(1):70–77
19. Qin GX, Jiang NY, Seo JH et al (2010) Cryogenic operation of a 24 GHz MMIC SiGe HBT medium power amplifier. Semicond Sci Technol 25(12):125002–125007
20. Çağlar A, Yelten MB (2016) Design of Cryogenic LNAs for High Linearity in Space Applications. IEEE Trans Circuits Syst I Regul Pap 66(12):4619–4627
21. Weinreb S, Shi J (2021) Low Noise Amplifier With 7-K Noise at 1.4 GHz and 25 ℃. IEEE Trans Microw Theory Tech 69(4):2345–2351
22. Zhou SH, Wang J (2022) An Experimental Investigation of the Degradation of CMOS Low-Noise Amplifier Specifications at Different Temperatures. Micromachines 13(8):1268–1277
23. Lin Q, Jia LN, Wu HF et al (2022) Investigation on Temperature Behavior for a GaAs E-pHEMT MMIC LNA. Micromachines 13(7):1121–1131
24. Chen CH, Deen MJ (1998) High frequency noise of MOSFETs I Modeling. Solid-State Electron 42(11):2069–2081
25. Magnone P, Petucco A, Thevenet N, Abedini H (2019) Simplified on-line monitoring system of MOSFET on-resistance based on a semi-empirical model",IEEE Applied Power Electronics Conference and Exposition (APEC). Anaheim, CA, USA, pp 2746–2750
26. Chen S, Yuan JS (2011) Adaptive gate bias for power amplifier temperature compensation. IEEE Trans Device Mater Reliab 11(3):442–449
27. Razavi B (2003) Design of Analog CMOS Integrated Circuits. McGraw Hill Higher Education, New York
28. Zhao H, Zhou SH, Nie MN (2021) Experimentally investigating the performance degradations of the CMOS PA at different temperatures. AIP Adv 11(11):115205–115212. https://doi.org/10.1063/5.0071801
29. Gray R, Hurst PJ, Lewis SH, Meyer RG (2001) Analysis and Design of Analog Integrated Circuits. Wiley, New York

Qian Lin received the B.S. degree Electronic Information science and technology from Qinghai Minzu University, Xining. China, in 2004,the M.S. degree Electronic Information science and technology from Qinghai Minzu University, Xining. China, in 2010, and the Ph.D. degree in circuits and systems from Tianjin University, Tianjin, China, in 2017. She is currently a professor with Qinghai Minzu University. Her research interests include the RF circuit design, 3-D modeling, testing, simulation of circuit reliability, and electronic technology applications.

Meiqian Wang is studing for the master degree in School of Physics and Electronic Information Engineering, Qinghai Minzu University. Her direction is the research temperature test of RF microwave power.